

## PHYSICS CONTRIBUTION

# REPOSITIONING ACCURACY OF TWO DIFFERENT MASK SYSTEMS—3D REVISITED: COMPARISON USING TRUE 3D/3D MATCHING WITH CONE-BEAM CT

JUDIT BODA-HEGGEMANN, M.D., PH.D.,\* CORNELIA WALTER, M.SC., ANGELIKA RAHN, M.D., HANSJÖRG WERTZ, M.SC., IRIS LOEB, B.SC., FRANK LOHR, M.D., AND FREDERIK WENZ, M.D.

\*Department of Radiation Oncology, Mannheim Medical Center, University of Heidelberg, Mannheim, Germany

**Purpose:** The repositioning accuracy of mask-based fixation systems has been assessed with two-dimensional/two-dimensional or two-dimensional/three-dimensional (3D) matching. We analyzed the accuracy of commercially available head mask systems, using true 3D/3D matching, with X-ray volume imaging and cone-beam CT.

**Methods and Materials:** Twenty-one patients receiving radiotherapy (intracranial/head-and-neck tumors) were evaluated (14 patients with rigid and 7 with thermoplastic masks). X-ray volume imaging was analyzed online and offline separately for the skull and neck regions. Translation/rotation errors of the target isocenter were analyzed. Four patients were treated to neck sites. For these patients, repositioning was aided by additional body tattoos. A separate analysis of the setup error on the basis of the registration of the cervical vertebra was performed. The residual error after correction and intrafractional motility were calculated.

**Results:** The mean length of the displacement vector for rigid masks was  $0.312 \pm 0.152$  cm (intracranial) and  $0.586 \pm 0.294$  cm (neck). For the thermoplastic masks, the value was  $0.472 \pm 0.174$  cm (intracranial) and  $0.726 \pm 0.445$  cm (neck). Rigid masks with body tattoos had a displacement vector length in the neck region of  $0.35 \pm 0.197$  cm. The intracranial residual error and intrafractional motility after X-ray volume imaging correction for rigid masks was  $0.188 \pm 0.074$  cm, and was  $0.134 \pm 0.14$  cm for thermoplastic masks.

**Conclusions:** The results of our study have demonstrated that rigid masks have a high intracranial repositioning accuracy per se. Given the small residual error and intrafractional movement, thermoplastic masks may also be used for high-precision treatments when combined with cone-beam CT. The neck region repositioning accuracy was worse than the intracranial accuracy in both cases. However, body tattoos and image guidance improved the accuracy. Finally, the combination of both mask systems with 3D image guidance has the potential to replace therapy simulation and intracranial stereotaxy. © 2006 Elsevier Inc.

Reproducibility, Positioning, Head mask, Cone-beam CT, Frameless stereotaxy.

## INTRODUCTION

Reliable and precise immobilization and accurate interfractional repositioning are of major importance in modern radiotherapy. Especially for high-precision techniques with steep dose gradients, such as intensity-modulated radiotherapy, heavy ion therapy, or radiosurgery with high radiation doses, the correct localization and positioning (1) of the isocenter is crucial to maintain the functions of the organs at risk in critical proximity to the target volume (2). Tumors in the cranial region are excellent candidates for precise repositioning, because they are not affected by organ movement and are stably correlated with bony structures. Patient fix-

ation in the cranial region has been performed with several established invasive and noninvasive devices (1).

Several minimally invasive (e.g., fixed pin systems [3, 4] and implanted fiducials [5, 6]) and noninvasive (e.g., maxillary [4] and dental [7] fixation, Laitinen's stereoadapter [noninvasive head frame] [8], and thermoplastic or vacuum-formed masks [9–13]) systems have been introduced. However, the comparison of the accuracy of these systems with a standardized protocol for testing and evaluation is missing (1), and, to date, peer-reviewed data are rare. Although these systems seem to work well in clinical practice, they may, nevertheless, exhibit a significant daily variation in target alignment. These uncertainties in mask systems can

Reprint requests to: Judit Boda-Heggemann M.D., Ph.D., Department of Radiation Oncology, Mannheim Medical Center, University of Heidelberg, Theodor-Kutzer Ufer 1-3, Mannheim 68167, Germany. Tel: (+49) 621-383-3530; Fax: (+49) 621-383-3493; E-mail: judit.boda-heggemann@radonk.ma.uni-heidelberg.de

Supported in part by a grant from Elekta, Crawley, UK, and

Nomos Corporation, Cranberry Township, PA.

**Acknowledgments**—We thank Petra Griess for expert application support with the pilot use of the XVI. We also thank Ute Köber and Sigrun Heidmann for excellent technical assistance with the XVI.

Received June 9, 2006, and in revised form Aug 21, 2006. Accepted for publication Aug 21, 2006.

result from different causes, such as weight changes of the patient (typically, weight loss for head-and-neck cancer patients and weight gain for those with intracerebral tumors receiving cortisone therapy), different mask-making techniques, or thermoplastic mask shrinking (10). Therefore, daily verification of the patient position may further enhance the precision of radiotherapy, depending on the system used.

The possible methods of testing the accuracy of different stereotactic systems include AP/lateral X-ray films, data from electronic portal imaging devices (EPID) compared with digitally reconstructed radiographs (14, 15) and video images, repeated CT or MRI scans outside the treatment room or using CT directly mounted to the linear accelerator (16). In some approaches, thermoplastic masks were compared with other systems using repeated CT images (10, 13). Using EPIDs, the repositioning accuracy of head and shoulder shells attached to a head board was studied (17). Rigid masks were analyzed using biplanar films (18). These data have shown that the different mask systems have a deviation of the isocenter position of several millimeters (18).

However, all the verification methods used to date have offered only two-dimensional (2D) or 2D/3D matching (19–22) to assess the repositioning accuracy, have been mostly accompanied by significant dose exposure to the patient, and, in the case of extra CT/MRI studies outside of the treatment room, have not been directly associated with the actual treatment.

Precise 3D visualization and localization of both cranial and extracranial targets is provided by techniques such as stand-alone treatment room CT (23, 24) or the gantry-mounted cone-beam (CB) approach (25). Kilovoltage CBCT implemented on board a linear accelerator offers the possibility of daily detection and correction of translational and rotational errors with a small dose exposure ( $\sim 0.9$  mGy [26, 27]) and good image quality. X-ray volume imaging (XVI) has an enormous potential to significantly improve the accuracy of radiotherapy. “On-board” linear accelerator-adapted CBCT is able to acquire multiple radiographs (in the case of head-and-neck imaging, approximately 350) immediately before a radiotherapy fraction within one 360° rotation of the gantry, with an acquisition time of 40 s to 1 min. The radiographs can be reconstructed with a back-projection algorithm to a volumetric image with a good spatial resolution of the soft tissues. This image can be compared with the planning image (CT) data set online and the patient position corrected if needed (25). The positioning error can be determined within six degrees of freedom, and the patient position can be immediately corrected; the number of degrees of freedom available for correction depends on the treatment table used.

The objective of this evaluation was to assess and compare the magnitude of the interfractional translational and rotational setup errors in two commercially available (rigid and thermoplastic) head mask systems with 3D data acquired using on-board CBCT, enabling a volume-based evaluation for the first time directly in the treatment room. Interfractional motion (28) and residual setup error were

also estimated. The data of both mask systems were analyzed online and offline separately for the intracranial and head-and-neck regions. Manual matching and automatic matching with a bone-matching algorithm were compared. Taken together, these data will provide a basis to assess the potential of on-board 3D image guidance to replace stereotactic methods.

## METHODS AND MATERIALS

### *Clinical setup and immobilization devices*

All 21 patients provided written informed consent for RT. Of the 21 patients, 14 were positioned using rigid masks (Delta Cast Elite) and 7 using thermoplastic masks. The Delta Cast Elite mask system (Leibinger, Freiburg, Germany) was used (18). The Delta Cast Elite consists of self-hardening bandages and is attached to a stereotactic frame (licensed production by Brandis Medizintechnik GmbH, Weinheim, Germany). The thermoplastic mask system (13) was obtained from Planet Medical GmbH (Hamburg, Germany). The masks are fixed to a carbon fiber baseplate that, in turn, is attached to the linear accelerator couch with three fixation points (Finesse System, Planet Medical, Svendborg, Denmark).

The patients were treated using a 6-MV linear accelerator (Elekta Synergy, Elekta, Crawley, UK). The patients were treated with intensity-modulated radiotherapy and/or 3D treatment plans with a stereotactic setup (Planning Systems, Corvus, NAS/Nomos, Cranberry Township, PA; OTP, Oncentra Masterplan, TheraNostic GmbH, Solingen, Germany). Before each treatment, the patients were positioned in either the rigid (Delta Cast Elite; Fig. 1a) or thermoplastic (Fig. 1b) mask system.

Of the 14 patients positioned in rigid masks and undergoing irradiation of head-and-neck tumors with a relevant tumor load in the neck region, 4 were positioned using body tattoos (sternum and left/right lateral thorax). A separate analysis of the setup error using registration of the cervical vertebra was performed. Four patients in rigid masks and two in thermoplastic masks were evaluated separately for residual error and intrafractional movement.

### *Planning CT*

Computed tomography data sets for treatment planning were acquired as a sequential scan with a slice thickness of 3 mm (VolumeZoom, Siemens, Erlangen, Germany).

### *Isocenter localization*

The patients underwent simulation or were positioned directly on the accelerator using stereotactic coordinates. Localization of

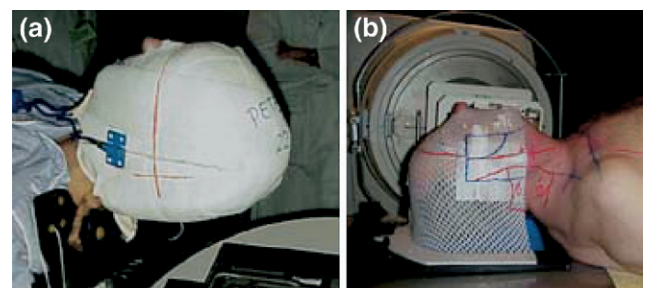


Fig. 1. (a) Rigid (Delta Cast Elite) and (b) thermoplastic mask systems.

the isocenter was verified by comparing the megavoltage EPIDs (iView GT, Elekta) or kilovoltage planar portal images (0° and 90°, XVI, Elekta) compared with digitally reconstructed radiographs generated by the treatment planning system. Isocenter localization was verified with 3D volume imaging using XVI. Patient position correction was then performed on the basis of the XVI, as described below.

### CB volume acquisition

Planning CT images, together with the organs at risk and planning target volume contours, were imported to the XVI control workstation (XVI software, version 3.5) from the planning system (OTP, Oncentra Masterplan, TheraNostic GmbH).

Daily CBCT volume scans were acquired for the two patient groups (Delta Cast Elite masks and thermoplastic masks), five times for each patient during their fractionated radiotherapy course. The projection images (~350) were acquired during a rotation of 284° in 47 s (in the case of head-and-neck imaging). The projections were processed with the Elekta XVI software. The accumulated dose was estimated to be ~0.9 mGy/acquisition as determined from measurements in the appropriate head phantom (29). This was a much smaller dose than that delivered by 0° and 90° megavoltage EPID imaging (40 mGy in the middle of a cylindrical phantom with a 20-cm diameter, T40015, PTW, Freiburg, Germany, and 50 mGy at the surface of the phantom, Walter C., personal communication, May 25, 2006). A back-projection algorithm with medium resolution (voxel size 1 mm<sup>3</sup>) was used to acquire the 3D volume images.

Planning CT images were matched online with the daily CT images using manual fusion independently by two different physicians or using the automatic bone-matching algorithm. The volume of interest for matching (“alignment clipbox”) was defined by the physicians. These alignment clipboxes were set for the intracranial region or on the neck vertebrae (Fig. 2) to allow for separate evaluation of the positioning in these regions.

On the basis of this matching, the translational and rotational positioning error (and, consequentially, the necessary isocenter shift for correction of this error) was calculated using the XVI

software. In addition to these online corrections and evaluations, the data were analyzed in a more detailed fashion offline. This offline analysis focused on the skull region or neck region and was performed by different physicians, as well as using an automatic bone-matching algorithm, with alignment clipboxes encompassing either the skull base or neck region (Fig. 2). The x (left–right), y (craniocaudal), and z (AP) components of translation of the target isocenter, the absolute target isocenter translation (total magnitude vector; “sum-vector”), and target isocenter rotation in the x, y, and z directions were documented and analyzed for each physician’s matching, as well as for the automatic registration.

An extensive quality assurance program assessed the image resolution, image distortion, and precision of isocenter detection on a weekly basis (29).

### Image analysis

The following analyses were performed:

1. 25 XVI scans for 5 patients were evaluated to estimate the repositioning accuracy of the thermoplastic masks in the intracranial region before any image-guided corrections.
2. 20 XVI scans of the same 4 patients (1 patient could not be evaluated in the neck region) were evaluated to estimate the repositioning accuracy of the thermoplastic masks in the neck region before any image-guided corrections.
3. 30 XVI scans for 6 patients were evaluated to estimate the repositioning accuracy of the rigid masks in the intracranial region before any image-guided corrections.
4. 30 XVI scans of the same 6 patients were evaluated to estimate the repositioning accuracy of the rigid masks in the neck regions before any image-guided corrections, if no body tattoos were used (no special efforts/other devices used to improve the repositioning accuracy in the neck region).
5. 13 XVI scans of 4 patients undergoing radiotherapy to the neck region were evaluated to estimate the repositioning accuracy of the rigid masks before any image-guided corrections combined with thoracic body tattoos in the neck region (special effort used to improve repositioning accuracy in the neck region).

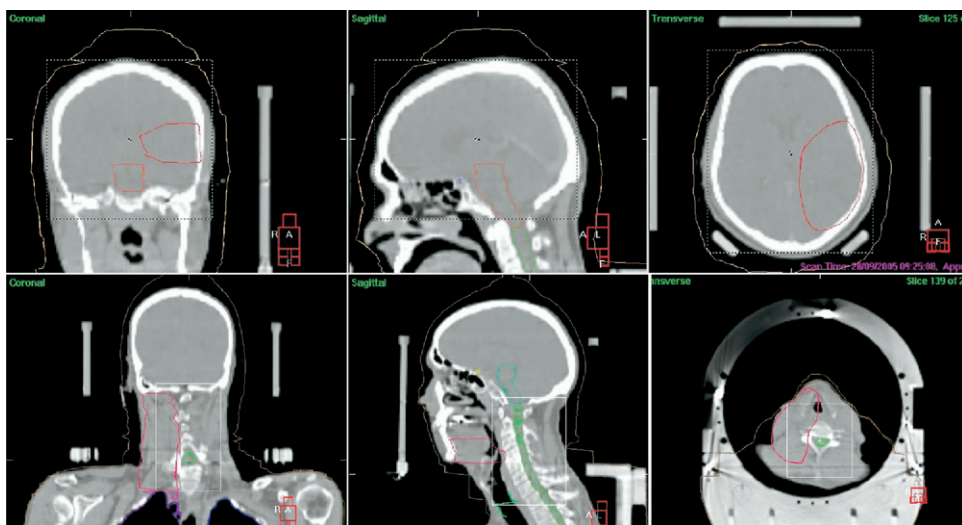


Fig. 2. Setup for alignment clipbox for automatic bone matching in intracranial region (upper images, skull–skull base) and neck region (lower images, cervical vertebrae) shown in planning CT data. Offline changing of alignment clipbox for evaluation of positioning in area not within immediate treatment area of patient is possible.



To ensure accurate positioning after translational table move corrections, the intrafractional movement and residual error were separately evaluated by acquiring CBCT scans in 4 patients with rigid masks (17 alignments) and 2 patients with thermoplastic masks (6 alignments) before and after radiotherapy sessions (after positioning correction with couch movements had been performed on the basis of the initial XVI volume data). Reposition errors and intrafractional position changes were estimated using CBCT correction after radiotherapy.

After immediate online correction, the CBCT data were analyzed offline by two physicians, and automatic bone matching was also performed with an alignment clipbox encompassing the intracranial region or neck region. The masks were tested for two different areas (intracranial or neck region) with changing of the alignment clipbox or the physician's personal region of interest.

### Data processing

The mean value and standard deviation of all translational and rotational errors were calculated for the matching results of each reader and for the automatic bone matching algorithm. The length of the translational correction vector was calculated using the following formula:  $v = \sqrt{(x^2 + y^2 + z^2)}$ . The residual error and intrafraction mobility after position correction using CB volume imaging was estimated based on results obtained with the automatic bone matching algorithm with an appropriate choice of the alignment clipbox position.

## RESULTS

### Analysis of isocenter position correction for rigid/stereotactic masks for intracranial region

A typical example for a rigid mask is shown in Fig. 3. Fig. 3a–c shows the position in the coronal, sagittal, and transversal directions before correction. Fig. 3d–f shows the position correction in the same directions by the physician considering the intracranial region.

An average of the isocenter translation corrections by a physician with the matching area restricted to the skull

region in the x, y, and z directions yielded a value of  $0.056 \pm 0.149$  cm,  $0.035 \pm 0.289$  cm, and  $-0.03 \pm 0.18$  cm, respectively. The length of the translation-vector (sum-vector) calculated from the x, y, and z corrections was  $0.311 \pm 0.21$  cm. The average isocenter rotation by the same examiner in the x, y, and z directions yielded  $-0.003^\circ \pm 1.074^\circ$ ,  $0.17^\circ \pm 1.39^\circ$ , and  $-0.07^\circ \pm 0.53^\circ$ , respectively.

The same corrections for the isocenter translation in x, y, and z directions by a second physician yielded  $0.02 \pm 0.13$  cm,  $0.077 \pm 0.263$  cm, and  $0.005 \pm 0.168$  cm, respectively. The translation-vector (sum-vector) calculated from the x, y, and z corrections was  $0.309 \pm 0.148$  cm. The rotation of the isocenter by this examiner in the x, y, and z directions was  $0.019^\circ \pm 0.994^\circ$ ,  $0.197^\circ \pm 1.09^\circ$ , and  $-0.01^\circ \pm 0.24^\circ$ , respectively.

Using automatic bone-matching corrections with an alignment clipbox respecting the skull (intracranial region) resulted in a translational correction in the x, y, and z directions of  $0.039 \pm 0.175$  cm,  $0.083 \pm 0.232$  cm, and  $0.005 \pm 0.174$  cm, respectively. The translation-vector (sum-vector) calculated from the x, y, and z corrections was  $0.312 \pm 0.152$  cm. The rotational correction in the x, y, and z directions with automatic bone matching was  $0.073^\circ \pm 1.018^\circ$ ,  $0.13^\circ \pm 1.653^\circ$ , and  $-0.25^\circ \pm 0.881^\circ$ , respectively.

With all three evaluations, the maximal standard deviation of the corrections in the x, y, and z directions was  $<1.75$  mm,  $<2.9$  mm, and  $<1.8$  mm, respectively. The rotational errors did not exceed  $1.07^\circ$ ,  $1.65^\circ$ , and  $0.88^\circ$  in the x, y, and z directions, respectively.

For each of these registrations, as well as the following data, the differences between alignments by the two physicians and automatic bone matching were  $<0.04$  cm, and  $<0.24^\circ$ . We have therefore only reported the results of the automatic bone matching.

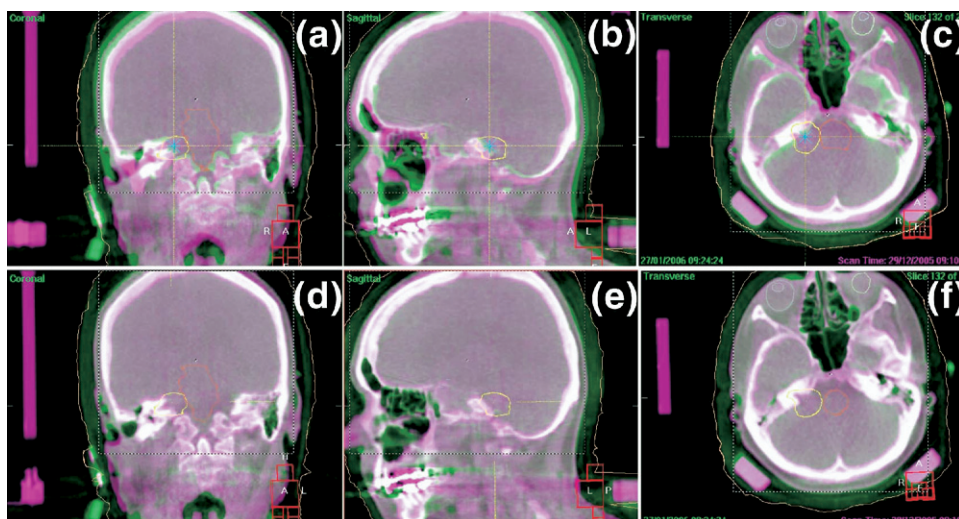


Fig. 3. Rigid mask, with registration for intracranial region by physician. Patient underwent radiotherapy for acoustic neuroma. Pink indicates planning CT; green, cone-beam CT. (a–c) Before correction; (d–f) after correction.

### *Analysis of isocenter position correction for thermoplastic masks for intracranial region*

Using automatic bone matching corrections with an alignment clipbox encompassing the skull (intracranial tumors) resulted in a translational correction in the x, y, and z directions of  $-0.02 \pm 0.227$  cm,  $0.23 \pm 0.233$  cm, and  $-0.154 \pm 0.277$  cm, respectively. The translation-vector (sum-vector) calculated from the x, y, and z corrections was  $0.472 \pm 0.174$  cm. The rotational correction in the x, y, and z directions with bone matching was  $-1.47^\circ \pm 1.75^\circ$ ,  $-0.13^\circ \pm 1.921^\circ$ , and  $-0.06^\circ \pm 2.18^\circ$ , respectively.

### *Analysis of isocenter position correction by rigid masks for neck region, without special effort for neck reposition accuracy*

For the group of intracranial tumor patients with rigid masks and without body tattoos for additional accuracy, the position correction was only performed offline and did not result in any additional position corrections because the neck was not relevant to the treatment. Patients irradiated in the neck region had body tattoos and were evaluated separately.

Using automatic bone matching corrections with an alignment clipbox encompassing the neck resulted in a translational correction in the x, y, and z directions of  $-0.158 \pm 0.207$  cm,  $0.225 \pm 0.241$  cm, and  $0.179 \pm 0.479$  cm, respectively. The correction vector calculated from the x, y, and z correction was  $0.586 \pm 0.294$  cm. The rotational correction in the x, y, and z directions was  $1.027^\circ \pm 3.527^\circ$ ,  $1.013^\circ \pm 2.556^\circ$ , and  $1.257^\circ \pm 3.008^\circ$ , respectively.

### *Analysis of isocenter position correction for rigid masks for neck region with body tattoos used to improve neck reposition accuracy*

Four patients with head-and-neck tumors were marked with body tattoos on the sternum and on the left and right side of the upper thorax at the planning CT. At every treatment session, the neck/thorax of the patients was positioned according to the body tattoos. These patients, be-

cause of their more precise positioning in the neck regions, were evaluated separately.

Using automatic bone matching corrections with an alignment clipbox encompassing the neck resulted in a translational correction in the x, y, and z directions of  $0.043 \pm 0.258$  cm,  $-0.04 \pm 0.191$  cm, and  $-0.08 \pm 0.241$  cm, respectively. The correction vector calculated from the x, y, and z correction was  $0.35 \pm 0.197$  cm. The rotational correction in the x, y, and z directions was  $-0.82^\circ \pm 1.298^\circ$ ,  $0.654^\circ \pm 1.059^\circ$ , and  $0.023^\circ \pm 1.204^\circ$ , respectively. The total length of the displacement vector was reduced compared with that for patients without body tattoos. The repositioning accuracy was still acceptable when body tattoos were used for the initial setup and could be reduced further by image-guided positioning correction.

### *Analysis of isocenter position correction for thermoplastic masks for neck region*

Using automatic bone matching corrections with an alignment clipbox respecting the neck (head-and-neck tumors) resulted in a translational correction in the x, y, and z directions of  $-0.205 \pm 0.298$  cm,  $0.407 \pm 0.516$  cm, and  $-0.142 \pm 0.393$  cm, respectively. The translational vector calculated from the x, y, and z corrections was  $0.726 \pm 0.445$  cm. The rotational correction in the x, y, and z directions was  $-0.2^\circ \pm 2.31^\circ$ ,  $-1.3^\circ \pm 2.69^\circ$ , and  $-1.09^\circ \pm 2.02^\circ$ , respectively. All results are summarized in Table 1.

### *Residual error and intrafractional position changes after CB correction*

The residual error and intrafractional position changes after CB correction regarding the intracranial region was evaluated using automatic bone matching for 2 patients in thermoplastic masks and 4 patients in rigid masks with one XVI after correction and delivering radiotherapy.

In the rigid masks, the translational correction in the x, y, and z directions was  $0.017 \pm 0.118$  cm,  $0.07 \pm 0.094$  cm, and  $-0.04 \pm 0.115$  cm, respectively. The translational vector calculated from the x, y, and z corrections

Table 1. Summary of results of repositioning errors using automatic bone matching

	Translation (cm)				Rotation ( $^\circ$ )		
	x	y	z	Vector (cm)	x	y	z
Intracranial							
Rigid masks	$0.039 \pm 0.175$	$0.083 \pm 0.232$	$0.005 \pm 0.174$	$0.312 \pm 0.152$	$0.073 \pm 1.018$	$0.13 \pm 1.653$	$-0.25 \pm 0.0881$
Thermoplastic masks	$-0.02 \pm 0.227$	$0.23 \pm 0.233$	$-0.154 \pm 0.277$	$0.472 \pm 0.174$	$-1.47 \pm 1.75$	$-0.13 \pm 1.921$	$-0.06 \pm 2.18$
Neck							
Rigid masks							
No tattoos	$-0.158 \pm 0.207$	$0.225 \pm 0.241$	$0.179 \pm 0.479$	$0.586 \pm 0.294$	$1.027 \pm 3.527$	$1.013 \pm 2.556$	$1.257 \pm 3.008$
Body tattoos	$0.043 \pm 0.258$	$-0.04 \pm 0.191$	$-0.08 \pm 0.241$	$0.35 \pm 0.197$	$-0.82 \pm 1.298$	$0.654 \pm 1.059$	$0.023 \pm 1.204$
Thermoplastic masks	$0.205 \pm 0.298$	$0.407 \pm 0.516$	$0.142 \pm 0.393$	$0.726 \pm 0.445$	$-0.2 \pm 2.31$	$-1.3 \pm 2.69$	$-1.09 \pm 2.02$

Data presented as mean  $\pm$  standard deviation.

was  $0.188 \pm 0.074$  cm. The rotational correction in the x, y, and z directions was  $-1.15^\circ \pm 1.045^\circ$ ,  $-0.1^\circ \pm 0.923^\circ$ , and  $-0.22^\circ \pm 0.717^\circ$ , respectively.

In the thermoplastic masks, the translational correction in the x, y, and z directions was  $0.04 \pm 0.14$  cm,  $0.033 \pm 0.145$  cm, and  $0.01 \pm 0.106$  cm, respectively. The translational vector calculated from the x, y, and z corrections was  $0.134 \pm 0.14$  cm. The rotational correction in the x, y, and z directions was  $-0.13^\circ \pm 1.206^\circ$ ,  $-0.13^\circ \pm 1.237^\circ$ , and  $0.08^\circ \pm 0.93^\circ$ , respectively.

## DISCUSSION

Fractionated radiotherapy has reached a high degree of accuracy with regard to image-based target definition (CT, MRI, positron emission tomography) and conformality (stereotactic radiosurgery, intensity-modulated radiotherapy [2]). Dose escalation may be advantageous for several intracranial and head-and-neck tumors (30, 31). The best treatment plan, however, is useless if patient/target positioning is not reliable. The repositioning accuracy of different, mostly mask-based, systems has been tested with 2D/2D (15–17, 32) and 2D/3D matching (18), which can be performed in the treatment room. However, for both approaches, the evaluation of rotational errors is not straightforward. Real 3D/3D matching outside the treatment room was performed by Fuss *et al.* (13). These data on different commercially available mask systems have shown a deviation in the isocenter position of several millimeters (results of studies summarized by Humphreys *et al.* [17]).

In this analysis, we performed an evaluation of the precision of different mask systems for the first time using real 3D/3D matching on the linear accelerator directly before radiotherapy with the help of CBCT.

With a mean length of the displacement vector of  $0.312 \pm 0.152$  cm intracranially and  $0.586 \pm 0.294$  cm in the neck and  $0.35 \pm 0.197$  cm without and with body tattoos, respectively, rigid mask systems per se provide excellent repositioning accuracy. Body tattoos reduced the positioning error in the neck region significantly, thus obviating the need for additional thoracic fixation. The advantage over thermoplastic masks is clear ( $0.472 \pm 0.174$  cm intracranially and  $0.726 \pm 0.445$  cm in the neck) and justifies the extra effort of manufacturing rigid masks if a stereotactic setup is used without 3D image guidance. The quality of the automatic bone-matching algorithm was emphasized by the excellent correlation between the manual matching and the automatic approach. When considering the data of the repositioning error plus the intrafractional movement, we acknowledge that patients undergoing radiotherapy in a rigid mask usually had treatment plans with a treatment duration of 20 min and several table angles such that the table was rotated several times during one fraction, which may have increased the intrafractional position changes by the minimal amount recorded in this analysis. Patients positioned with thermoplastic masks were treated with fewer table angles. This might explain why patients positioned with thermoplastic masks had

even smaller intrafractional movement detected than that detected in patients with rigid masks.

With values of 1–2 mm for both rigid and thermoplastic mask systems, the intrafraction motion (28) can be considered negligible for awake and cooperative patients.

An issue of great importance is the combined error resulting from the residual error after image-guided positioning correction and intrafractional movement. That it was  $<2$  mm intracranially for both mask systems provides a rationale to forego stereotactic setup in the future and switch to a purely image-guided setup for all intracranial precision radiotherapy procedures. This could reduce the time needed ( $\leq 20$  min) for the personnel and patient in the head mask. That the combination of intrafractional movement/residual error was  $<2$  mm even for thermoplastic masks indicates that performing “stereotactic grade” procedures using these masks under image guidance is justified if patients do not tolerate the rigid mask. CBCT, therefore, also offers the possibility, in several situations, to forego conventional simulation. If positioning is extremely critical, it can be verified daily and, if necessary, can be corrected before each treatment session. An accelerated systematic workflow using image-guided radiotherapy is proposed in Fig. 4.

Another advantage of soft-tissue-based volume image guidance is that changes in patient anatomy/facial contours during radiotherapy, such as tissue loss (cachexia in patients with head-and-neck cancer treated with radiochemotherapy, neck volume loss because of tumor regression) or swelling (intracranial lesions treated with steroids) can be followed and accounted for by online correction and, if necessary, manufacturing a new mask and acquiring a new planning CT with subsequent modification of the treatment plan (33). This allows for better organ sparing, such as parotid sparing during head-and-neck radiation (34).

Another interesting issue is the question of additional dose accumulation because of image guidance. To date, the accuracy of different stereotactic systems has been assessed with biplanar (AP/lateral) X-ray films (18), EPIDs (17)

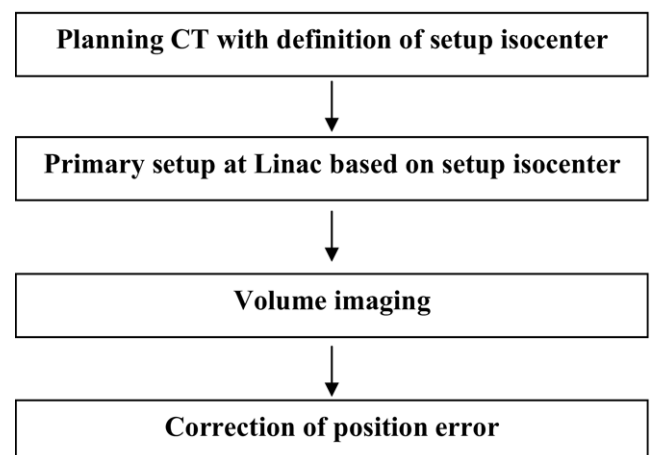


Fig. 4. Workflow for cranial precision radiotherapy by image-guided radiotherapy.

compared with digitally reconstructed radiographs (14), digitally reconstructed radiographs and video images, and repeated CT or MRI scans outside the treatment room (10, 13). All these verification methods result in different dose exposures to the patient. On the basis of recent data from our, and other groups (26, 34), kilovoltage planar imaging and kilovoltage volume imaging compare very favorably with megavoltage planar imaging.

In summary, volume imaging with CBCT has several advantages for verification of the patient position, including the ability to localize the patient contours and treatment isocenter in the actual therapy position; the possibility of correcting position errors in six degrees of freedom immediately if a treatment table capable of this performance, such as the HexaPOD (HexaPOD RTC, Medical Intelligence, Schwabmünchen, Germany) is available; low additional dose accumulation resulting from image guidance (same or less than that with two orthogonal megavoltage EPID pictures); minimal additional time and inconvenience for patient and personnel with additional potential for shortening time needed; given the small residual error after position correction, it is not necessary to perform CBCT again after correction (such as is usually done when 2D procedures such as megavoltage EPID are performed); and alignment can be focused on the area of interest, such as the skull and skull base region or the neck. This matching offers high accuracy and fast and precise verification of the patient position.

The commercial introduction of linear accelerator-adapted CBCT is a promising approach for the daily verification of patient positioning in cranial and extracranial precision radiotherapy (25, 35). Using CBCT will obviate simulation, the present generation of 2D verification methods, and stereotaxy in many clinical situations.

## CONCLUSION

The results of this study have demonstrated that rigid masks have a high intracranial repositioning accuracy per se. Their combination with 3D image guidance has the potential to replace intracranial stereotaxy.

However, thermoplastic masks were shown to be more precise than assumed and, because of the small rotational error and according to the data regarding residual error after position correction and regarding intrafractional movement, may be used for precision treatments when combined with CBCT.

The precision in the case of the neck region was, in both cases, worse than in the intracranial regions. The total length of the displacement vector, however, was still acceptable when body tattoos were used for the initial setup and could be further reduced using image-guided position corrections. Changes in patient anatomy or facial contours during radiotherapy can be detected early and appropriate action taken early in the treatment course.

## REFERENCES

- Lightstone AW, Benedict SH, Bova FJ, *et al.* Intracranial stereotactic positioning systems: Report of the American Association of Physicists in Medicine Radiation Therapy Committee Task Group No. 68. *Med Phys* 2005;32:2380–2398.
- Breen SL, Craig T, Bayley A, *et al.* Spinal cord planning risk volumes for intensity-modulated radiation therapy of head-and-neck cancer. *Int J Radiat Oncol Biol Phys* 2006;64:321–325.
- Ertl A, Saringer W, Heimberger K, *et al.* Quality assurance for the Leksell gamma unit: Considering magnetic resonance image-distortion and delineation failure in the targeting of the internal auditory canal. *Med Phys* 1999;26:166–170.
- Bale RJ, Voge M, Freysinger W, *et al.* Minimally invasive head holder to improve the performance of frameless stereotactic surgery. *Laryngoscope* 1997;107:373–377.
- Gall KP, Verhey LJ, Wagner M. Computer-assisted positioning of radiotherapy patients using implanted radiopaque fiducials. *Med Phys* 1993;20:1153–1159.
- Salter BJ, Fuss M, Vollmer DG, *et al.* The TALON removable head frame system for stereotactic radiosurgery/radiotherapy: Measurement of the repositioning accuracy. *Int J Radiat Oncol Biol Phys* 2001;51:555–562.
- Baumert BG, Egli P, Studer S, *et al.* Repositioning accuracy of fractionated stereotactic irradiation: Assessment of isocentre alignment for different dental fixations by using sequential CT scanning. *Radiother Oncol* 2005;74:61–66.
- Delannes M, Daly NJ, Bonnet J, *et al.* Fractionated radiotherapy of small inoperable lesions of the brain using a non-invasive stereotactic frame. *Int J Radiat Oncol Biol Phys* 1991;21:749–755.
- Willner J, Hädinger U, Neumann M, *et al.* Three dimensional variability in patient positioning using bite block immobilization in 3D-conformal radiation treatment for ENT-tumors. *Radiother Oncol* 1997;43:315–321.
- Tsai JS, Engler MJ, Ling MN, *et al.* A non-invasive immobilization system and related quality assurance for dynamic intensity modulated radiation therapy of intracranial and head and neck disease. *Int J Radiat Oncol Biol Phys* 1999;43:455–467.
- Thornton AF Jr, Ten Haken RK, Weeks KJ, *et al.* A head immobilization system for radiation simulation, CT, MRI, and PET imaging. *Med Dosim* 1991;16:51–56.
- Thornton AF Jr, Ten Haken RK, Gerhardtsson A, *et al.* Three-dimensional motion analysis of an improved head immobilization system for simulation, CT, MRI, and PET imaging. *Radiother Oncol* 1991;20:224–228.
- Fuss M, Salter BJ, Cheek D, *et al.* Repositioning accuracy of a commercially available thermoplastic mask system. *Radiother Oncol* 2004;71:339–345.
- Lohr F, Schramm O, Schraube P, *et al.* Simulation of 3D-treatment plans in head and neck tumors aided by matching of digitally reconstructed radiographs (DRR) and on-line distortion corrected simulator images. *Radiother Oncol* 1997;45:199–207.
- Donato K, Leszczynski K, Fleming K. A comparative evaluation of two head and neck immobilization devices using electronic portal imaging. *Br J Radiol* 2006;79:158–161.
- de Boer HC, van Sornsens de Koste JR, Creutzberg CL, *et al.* Electronic portal image assisted reduction of systematic set-up errors in head and neck irradiation. *Radiother Oncol* 2001;61:299–308.
- Humphreys M, Guerrero Urbano MT, Mubata C, *et al.* Assessment of a customised immobilisation system for head and neck



- IMRT using electronic portal imaging. *Radiother Oncol* 2005;77:39–44.
18. Karger CP, Jakel O, Debus J, *et al.* Three-dimensional accuracy and interfractional reproducibility of patient fixation and positioning using a stereotactic head mask system. *Int J Radiat Oncol Biol Phys* 2001;49:1493–1504.
  19. Gilhuijs KG, Touw A, van Herk M, *et al.* Optimization of automatic portal image analysis. *Med Phys* 1995;22:1089–1099.
  20. Gilhuijs KG, van de Ven PJ, van Herk M. Automatic three-dimensional inspection of patient setup in radiation therapy using portal images, simulator images, and computed tomography data. *Med Phys* 1996;23:389–399.
  21. Gilhuijs KG, Drukker K, Touw A, *et al.* Interactive three dimensional inspection of patient setup in radiation therapy using digital portal images and computed tomography data. *Int J Radiat Oncol Biol Phys* 1996;34:873–885.
  22. van Herk M, Bel A, Gilhuijs KG, *et al.* Electronic portal imaging. *Bull Cancer* 1995;82(Suppl. 5):601s–606s.
  23. Hof H, Herfarth KK, Munter M, *et al.* The use of the multi-slice CT for the determination of respiratory lung tumor movement in stereotactic single-dose irradiation. *Strahlenther Onkol* 2003;179:542–547.
  24. Uematsu M, Shioda A, Suda A, *et al.* Intrafractional tumor position stability during computed tomography (CT)-guided frameless stereotactic radiation therapy for lung or liver cancers with a fusion of CT and linear accelerator (FOCAL) unit. *Int J Radiat Oncol Biol Phys* 2000;48:443–448.
  25. Jaffray DA, Siewerdsen JH, Wong JW, *et al.* Flat-panel cone-beam computed tomography for image-guided radiation therapy. *Int J Radiat Oncol Biol Phys* 2002;53:1337–1349.
  26. Walter C, Boda-Heggemann J, Wertz H, Rahn A, Lohr F, Wenz F. *In vivo* dose measurements of extra dose from cone-beam computed tomography [Letter]. *Int J Radiat Oncol Biol Phys* 2006;66:632
  27. Walter C, Boda-Heggemann J, Wertz H, *et al.* In-vivo Messungen zur Dosisbelastung bei der Bildgebung am Linearbeschleuniger durch portal images und Cone-beam-CT. *Strahlenther Onkol* 2006;182(Suppl. 1):117.
  28. Linthout N, Verellen D, Tournel K, *et al.* Six dimensional analysis with daily stereoscopic x-ray imaging of intrafraction patient motion in head and neck treatments using five points fixation masks. *Med Phys* 2006;33:504–513.
  29. Walter C, Wertz H, Steil V, *et al.* Messungen zur Qualitätssicherung am Cone-beam CT. *Strahlenther Onkol* 2006;182(Suppl. 1):95.
  30. Odrzka K, Petera J, Zouhar M, *et al.* Clinical results of intensity-modulated radiation therapy (IMRT) for tumors of the head and neck region. *Neoplasma* 2005;52:85–94.
  31. Shrieve DC, Tarbell NJ, Alexander E III, *et al.* Stereotactic radiotherapy: A technique for dose optimization and escalation for intracranial tumors. *Acta Neurochir Suppl* 1994;62:118–123.
  32. Gilbeau L, Octave-Prignot M, Loncol T, *et al.* Comparison of setup accuracy of three different thermoplastic masks for the treatment of brain and head and neck tumors. *Radiother Oncol* 2001;58:155–162.
  33. Hansen EK, Bucci MK, Quivey JM, *et al.* Repeat CT imaging and replanning during the course of IMRT for head-and-neck cancer. *Int J Radiat Oncol Biol Phys* 2006;64:355–362.
  34. McMillan AS, Pow EH, Kwong DL, *et al.* Preservation of quality of life after intensity-modulated radiotherapy for early-stage nasopharyngeal carcinoma: Results of a prospective longitudinal study. *Head Neck* 2006;28:712–722.
  35. McBain CA, Henry AM, Sykes J, *et al.* X-ray volumetric imaging in image-guided radiotherapy: The new standard in on-treatment imaging. *Int J Radiat Oncol Biol Phys* 2006;64:625–634.